Communication

Manganese-Based Nanoscale Metal#Organic Frameworks for Magnetic Resonance Imaging

Kathryn M. L. Taylor, William J. Rieter, and Wenbin Lin

J. Am. Chem. Soc., **2008**, 130 (44), 14358-14359 • DOI: 10.1021/ja803777x • Publication Date (Web): 10 October 2008

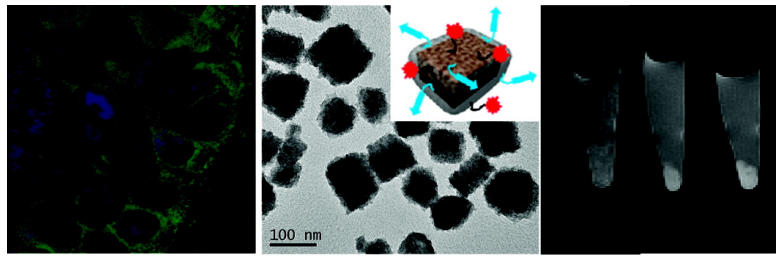

J|A|C|S
COMMUNICATIONS

Published on Web 10/10/2008

Manganese-Based Nanoscale Metal−Organic Frameworks for Magnetic Resonance Imaging

Kathryn M. L. Taylor, William J. Rieter, and Wenbin Lin*

Department of Chemistry, CB#3290, University of North Carolina, Chapel Hill, North Carolina 27599

Received May 20, 2008; E-mail: wlin@unc.edu

Magnetic resonance imaging (MRI) is a powerful noninvasive diagnostic tool that provides high spatial resolution images and does not involve radioactivity.[1] Intrinsically low sensitivity of MRI however necessitates the use of contrast agents that are often administered in high doses.[2] Paramagnetic and superparamagnetic nanomaterials have recently emerged as promising MR contrast agents owing to their ability to carry large payloads of magnetic centers.[3] They can work at very low concentrations and be made target-specific by conjugation with affinity molecules.[4]

We recently demonstrated the synthesis of Gd-based nanoscale metal−organic frameworks (NMOFs) with extraordinarily high MR relaxivities on a per particle basis. The toxicity of leached Gd^{3+} ions however precludes clinical applications of these NMOFs. Given the modular nature of MOFs, their compositions and structures can be readily tuned by a judicious choice of metal ions and organic linkers to lead to MR-enhancing NMOFs that are more biocompatible and less toxic. Indeed, Mn^{2+} centers are much less toxic than Gd^{3+} centers and have been shown to exhibit very high in vivo longitudinal (r_1) MR relaxivities by binding to intracellular proteins.[5] Herein we wish to report the synthesis of Mn NMOFs, their coating with a thin silica shell, and subsequent functionalization with a cyclic arginine−glycine−aspartate (RGD) peptide and a fluorophore, and the application of such core−shell nanostructures in MR imaging.

Mn NMOFs with terephthalic acid (BDC) and trimesic acid (BTC) bridging ligands were synthesized in reverse-phase microemulsions.[6] Nanorods of $Mn(BDC)(H_2O)_2$ (**1**) were synthesized by stirring a CTAB/1-hexanol/*n*-heptane/water microemulsion with a *W*-value of 5 that contained equal molar $MnCl_2$ and $[NMeH_3]_2(BDC)$ for 18 h at room temp. SEM and TEM micrographs show that particles of **1** adopt a rodlike morphology with diameters of 50−100 nm and lengths of 750 nm to several μm (Figure 1). Powder X-ray diffraction (PXRD) studies indicated that nanorods of **1** are crystalline and correspond to the known bulk phase of $Mn(BDC)(H_2O)_2$.[7] The composition was also confirmed by TGA and ICP−MS results.

Nanoparticles of $Mn_3(BTC)_2(H_2O)_6$, **2**, were similarly prepared in a CTAB/1-hexanol/isooctane/water microemulsion ($W = 10$) with a $Na_3(BTC)/MnCl_2$ molar ratio of 2:3. SEM and TEM micrographs show that particles of **2** are fairly uniform and adopt an unusual spiral rod morphology with diameters of 50−100 nm and lengths of 1−2 μm (Figure 2a,b).[8] The spiral nanorods are crystalline based on PXRD but do not correspond to any known phase of Mn-BTC MOFs.[9] The composition of **2** was established on the basis of TGA and ICP−MS results.

We also carried out surfactant-assisted synthesis of **1** and **2** under microwave heating in an attempt to alter their morphologies. Nanorods of **1** were obtained after heating a CTAB/1-hexanol/*n*-heptane/water microemulsion of $MnCl_2$ and $[NMeH_3]_2(BDC)$ in 1:1 molar ratio with a *W*-value of 10 at 120 °C for 10 min in an 800 W microwave. SEM, PXRD, and TGA studies showed that nanorods of **1** obtained under microwave heating have identical phase and similar morphology to those obtained from the room temperature reaction. Interestingly,

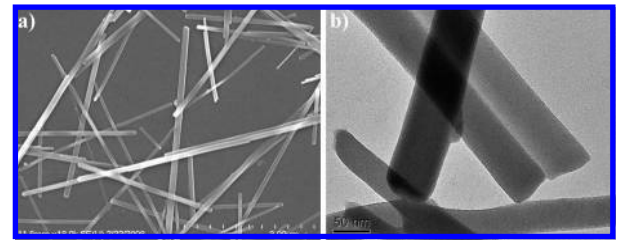

Figure 1. SEM (a) and TEM (b) images of $Mn(BDC)(H_2O)_2$ nanorods (**1**).

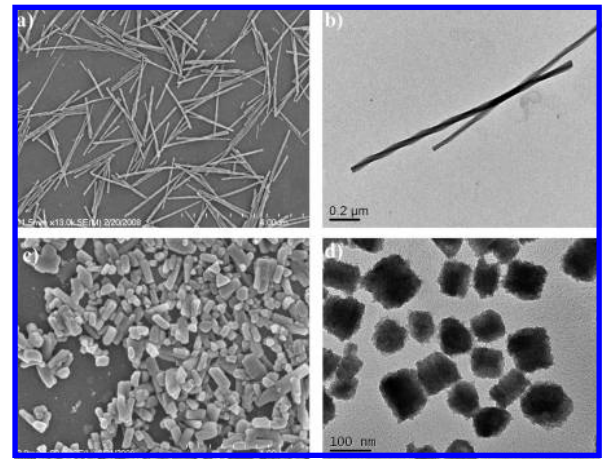

Figure 2. SEM (a) and TEM (b) images of $Mn_3(BTC)_2(H_2O)_6$ spiral nanorods (**2**) synthesized at room temp; (c) SEM image of nanoparticles of **2** synthesized at 120 °C under microwave heating; (d) TEM image of silica-coated nanoparticles of **2** that were under microwave heating.

microwave heating of a CTAB/1-hexanol/isooctane/water microemulsion of $Na_3(BTC)$ and $MnCl_2$ (in 2:3 molar ratio) with a *W*-value of 10 at 120 °C for 10 min produced nanoparticles of **2** with a much lower aspect ratio. PXRD and TGA indicated that nanoparticles of **2** obtained under microwave heating are the same phase as those obtained at room temperature, but SEM and TEM images showed that the particles obtained under microwave heating have a blocklike morphology, with lengths ranging from ~50 to 300 nm in the three dimensions (Figure 2c).

Microwave-synthesized nanoparticles of **2** were coated with a thin silica shell (denoted as **2′**) to stabilize them and to facilitate their functionalization with a fluorophore and a cell-targeting peptide. Nanoparticles of **2′** were prepared by base-catalyzed condensation of TEOS on PVP-modified particles of **2** in ethanol (Scheme 1).[10] TEM images indicated the presence of a thin shell of amorphous silica on **2′** (Figure 2d), which was confirmed by TGA since **2′** had an additional 7.1% weight remaining after heating at 600 °C in air. Rhodamine B and c(RGDfK) were grafted onto **2′** by treatment with RITC-APS (1.5 wt %) and tri(ethoxy)silylpropyl carbomoyl c(RGDfK) (~10 wt %) in a basic ethanolic suspension. Rhodamine B provides characteristic fluorescence for optical imaging whereas c(RGDfK) is a small cyclic

10.1021/ja803777x CCC: $40.75

Scheme 1

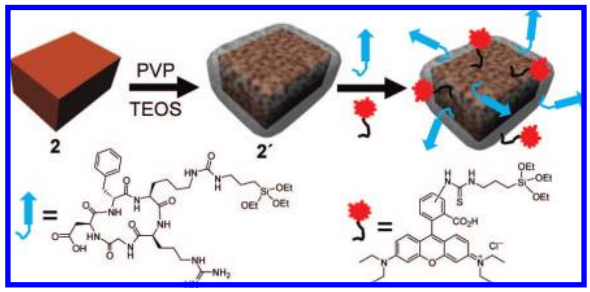

peptide that can target angiogenic cancers (such as HT-29) by binding to the upregulated $\alpha_v\beta_3$ integrin.

We determined MR relaxivities of **1** and **2** on a 3 T scanner. Nanorods of **1** were found to have a longitudinal relaxivity (r_1) of 5.5 and a transverse relaxivity (r_2) of 80.0 mM^{-1} s^{-1} on a per Mn basis, whereas nanorods of **2** exhibited an r_1 of 7.8 and an r_2 of 70.8 mM^{-1} s^{-1} on a per Mn basis. Consistent with this, nanorods of **2** had an r_1 of 4.6 and an r_2 of 141.2 mM^{-1} s^{-1} on a per Mn basis at 9.4 T. **2′** has slightly lower r_1 of 4.0 and r_2 of 112.8 mM^{-1} s^{-1} at 9.4 T. The slight decrease of MR relaxivities is expected because of the reduced influence of the Mn centers on the surrounding water molecules.

The r_1 values exhibited by the Mn NMOFs are modest and these nanoparticles are not expected to be efficient T_1-weighted contrast agents. Given the typically high water solubility of most MOFs, we hypothesized that the NMOFs might provide an efficient vehicle for the delivery of large doses of Mn^{2+} ions which are known to exhibit very high r_1 values inside cells.[5] Leaching studies indicated that **2′** has a half-life of 7.5 h (i.e., about ~50% Mn^{2+} ions were released from **2′**) whereas uncoated **2** has a half-life of 3.5 h in water at 37 °C (Figure 3a). In PBS buffer at 37 °C, the half-lives for **2** and **2′** were reduced to 18 min and 1.44 h, respectively. These results indicate the stabilization of the Mn NMOFs by silica coatings and suggest that the silica-coated particles should have adequate time to reach the site of interest where they will then release Mn^{2+} to give T_1-weighted contrast enhancement.

We evaluated the efficacy of **2′** that have been surface-functionalized with rhodamine B and c(RGDfK) as MR and optical contrast agents in vitro. Human colon cancer (HT-29) cells were incubated with rhodamine B-functionalized nanoparticles of **2′** with and without the c(RGDfK) targeting peptide. In vitro MR imaging of HT-29 cells showed the selective uptake of **2′** and thus the intracellular delivery of Mn^{2+} ions. As shown in Figure 3b, the HT-29 cells incubated with the targeted particles gave much higher signals in T_1-weighted images than those that were not incubated with nanoparticles as well as those that were incubated with the nontargeted particles. ICP−MS analysis supported the enhanced uptake of **2′** by HT-29 cells: the cell pellets (~3.2 million cells) contained 0.05, 0.33, and 2.29 μg of Mn after incubating with no particles, nontargeted **2′**, and targeted **2′**, respectively. Confocal microscopic imaging studies further confirmed the enhanced uptake of the particles with the targeting peptide, compared to those without the targeting peptide (Figure 3c,d). These results demonstrate the target-specific uptake of the c(RGDfK)-modified Mn NMOFs by angiogenic cancer cells, presumably via receptor-mediated endocytosis. Finally, we also demonstrated the in vivo utility of Mn NMOFs for Mn^{2+} ion delivery. T_1-weighted contrast enhancement was observed in the mouse liver, kidneys, and aorta ~1 h after tail vein injection of **2′** at a 10 μmol/kg Mn dose (Supporting Information), apparently caused by the Mn^{2+} ions released from the nanoparticles.

In summary, we have synthesized Mn NMOFs with controllable morphologies and demonstrated their potential for MR contrast

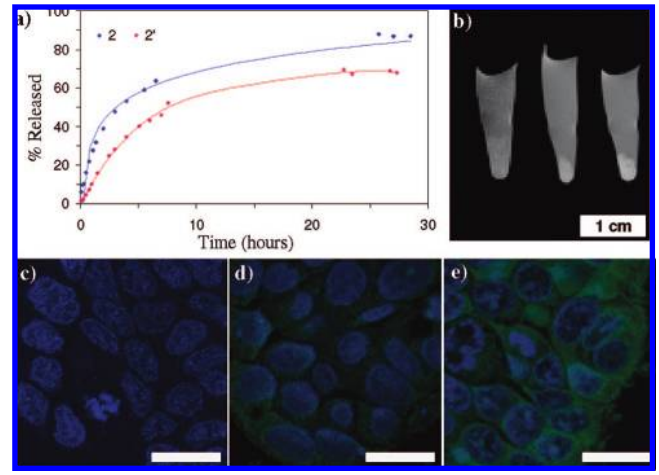

Figure 3. (a) Dissolution curves of uncoated (blue) and silica-coated (red) $Mn_3(BTC)_2(H_2O)_6$ nanoparticles (**2** and **2′**) in water at 37 °C (% released vs time). (b) In vitro MR images of HT-29 cells incubated with no **2′** (left), nontargeted **2′** (middle), and c(RGDfK)-targeted **2′** (right). (c−e) Merged confocal images of HT-29 cells that were incubated with no **2′** (c), nontargeted **2′** (d), c(RGDfK)-targeted **2′** (e). The blue color was from DRAQ5 used to stain the cell nuclei while the green color was from rhodamine B. The bars represent 20 μm.

enhancement. Surface functionalization of the Mn NMOFs with a cell-targeting molecule enhances their delivery to cancer cells to allow for target-specific MR imaging. Such a core−shell nanostructure platform can be used for targeted delivery of other imaging and therapeutic agents.

Acknowledgment. We acknowledge financial support from NIH (Grant U54-CA119343) and NSF. W.J.R. thanks NSF for a graduate fellowship. We thank Dr. Jason S. Kim, Dr. Hongyu An, and Mr. Joe Della Rocca for experimental help.

Supporting Information Available: Experimental procedures and 30 figures. This material is available free of charge via the Internet at http://pubs.acs.org.

References

(1) Stark, D. D.; Bradley, W. G., Jr. *Magnetic Resonance Imaging* Mosby: St. Louis, MO, 1999.
(2) (a) Toth, É.; Helm, L.; Merbach, A. E. *The Chemistry of Contrast Agents in Medical Magnetic Resonance Imaging;* John Wiley & Sons: Chichester, U.K., 2001. (b) Caravan, P.; Ellison, J. J.; McMurry, T. J.; Lauffer, R. B. *Chem. Rev.* **1999**, *99*, 2293.
(3) (a) Morawski, A. M.; Lanza, G. A.; Wickline, S. A. *Curr Opin. Biotechnol.* **2005**, *16*, 89. (b) Weissleder, R.; Moore, A.; Mahmood, U.; Bhorade, R.; Benveniste, H.; Chiocca, E. A.; Basilion, J. P. *Nat. Med.* **2000**, *6*, 351. (c) Na, H. B.; Lee, J. H.; An, K.; Park, Y. I; Park, M.; Lee, I. S.; Nam, D.-H.; Kim, S. T.; Kim, S.-H.; Kim, S.-W.; Lim, K.-H.; Kim, K.-S.; Kim, S.-O.; Hyeon, T. *Angew. Chem., Int. Ed.* **2007**, *46*, 5397. (d) Seo, W. S.; Lee, J. H.; Sun, X.; Suzuki, Y.; Mann, D.; Liu, Z.; Terashima, M.; Yang, P. C.; McConnell, M. V.; Nishimura, D. G.; Dai, H. *Nat. Mater.* **2006**, *5*, 971. (e) Rieter, W. J.; Kim, J. S.; Taylor, K. M. L.; An, H.; Lin, W.; Tarrant, T.; Lin, W. *Angew. Chem., Int. Ed.* **2007**, *46*, 3680. (f) Taylor, K. M. L.; Kim, J. S.; Rieter, W. J.; An, H.; Lin, W.; Lin, W. *J. Am. Chem. Soc.* **2008**, *130*, 2154.
(4) Kim, J. S.; Rieter, W. J.; Taylor, K. M. L.; An, H.; Lin, W.; Lin, W. *J. Am. Chem. Soc.* **2007**, *129*, 8962.
(5) Elizondo, G.; Fretz, C. J.; Stark, D. D.; Rocklage, S. M.; Quay, S. C.; Worah, D.; Tsang, Y-M.; Chen, M. C-M.; Ferrucci, J. T. *Radiology* **1991**, *178*, 73.
(6) Rieter, W. J.; Taylor, K. M. L.; An, H.; Lin, W.; Lin, W. *J. Am. Chem. Soc.* **2006**, *128*, 9024.
(7) Kaduk, J. A. *Acta Crystallogr., B* **2002**, *58*, 815.
(8) Coordination unsaturation for the Mn ions near the surface can induce strain in the system which might be responsible for the spiral morphology.
(9) We failed to grow single crystals of **2** for structure determination after numerous attempts. (a) Gutschke, S. O. H.; Molinier, M.; Powell, A. K.; Winpenney, R. E. P.; Wood, P. T. *Chem Commun.* **1996**, 823. (b) Chen, J.; Ohba, M.; Kitagawa, S. *Chem. Lett.* **2006**, *35*, 526.
(10) Rieter, W. J.; Taylor, K. M.; Lin, W. *J. Am. Chem. Soc.* **2007**, *129*, 9852.

JA803777X